

An Unusually Weak Intervalence Transition in a Very Stable Bis-Chelate Analogue of the Mixed-Valent Creutz–Taube Ion. UV/Vis/Near-IR and EPR Spectroelectrochemistry of $[(\text{NH}_3)_4\text{Ru}(\mu\text{-bptz})\text{Ru}(\text{NH}_3)_4]^{n+}$ (bptz = 3,6-Bis(2-pyridyl)-1,2,4,5-tetrazine; $n = 3\text{--}5$)

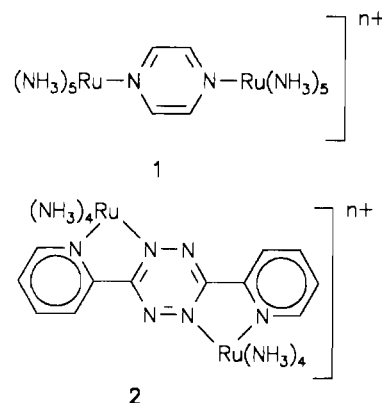
Jürgen Poppe, Michael Moscherosch, and Wolfgang Kaim*

Institut für Anorganische Chemie, Universität Stuttgart, Pfaffenwaldring 55, D-7000 Stuttgart 80, Germany

Received November 11, 1992

The pentacationic form 2^{5+} of the title complex, which exhibits an electrochemical stability constant K_c of 10^{15} in acetonitrile, shows much formal similarity to the mixed-valent (Ru^{II}/Ru^{III}) pyrazine-bridged Creutz–Taube ion 1^{5+} . However, the flanking of the central π -accepting tetrazine ring of the bridging ligand bptz by two coordinating pyridyl groups results in a rigid chelate arrangement with the ruthenium–ammine bonds situated parallel and perpendicular to the π system of bptz. This conformation is essentially different from the “staggered” arrangement in 1^{5+} , the difference being reflected not by the shape or maximum of the band due to the intervalence transition (IT) at 1450 nm but by a decrease of its intensity by 1 order of magnitude from ϵ 5000 (1^{5+}) to 500 $\text{M}^{-1} \text{cm}^{-1}$ for 2^{5+} . While the IT band maximum is essentially solvent insensitive, the near-IR spectrum in $\text{D}_2\text{O}/\text{DCl}$ reveals some structuring of the IT band with a spacing of about 900 cm^{-1} . In addition to UV/vis/near-IR spectroelectrochemistry, the EPR data confirm the metal-based spin in the $5+$ form ($g_1 = 2.019$, $g_2 = 2.418$, $g_3 = 2.913$) and a predominantly ligand-centered unpaired electron in the $3+$ state ($g_{\parallel} = 2.022$, $g_{\perp} = 1.989$), which is accessible here due to the good π -acceptor properties of bptz. Nevertheless, the observability of the EPR signal only below 70 K indicates a stronger metal contribution in 2^{3+} than in the related radical complex $[(\text{bpy})_2\text{Ru}(\mu\text{-bptz})\text{Ru}(\text{bpy})_2]^{3+}$.

Experimental studies in the field of mixed-valence coordination chemistry¹ have been dominated for some time by ruthenium-(II/III) ammine complexes,^{1,2} most of them modeled after the pyrazine-bridged Creutz–Taube ion 1^{5+} .^{2,3} In addition to the question of valence localization or delocalization, much of the research has focused on the understanding of spectral properties, especially of the characteristic long-wavelength metal-to-metal charge-transfer (MMCT) or intervalence transitions (IT),^{1,4} on the basis of theoretical models.⁵ Within our attempts to broaden the experimental basis of mixed-valence chemistry by introducing new bridging ligands⁶ and organometallic complex fragments⁷ related to $[\text{Ru}(\text{NH}_3)_3]^{2+/3+}$, we have now studied the optical and EPR spectral properties of odd-electron states of $[\mu\text{-3,6-bis(2-pyridyl)-1,2,4,5-tetrazine}]$ bis(pentaammineruthenium) (2^{n+}).

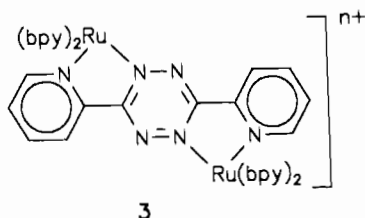


Complexes 2^{n+} contain the unique bridging ligand 3,6-bis(2-pyridyl)-1,2,4,5-tetrazine, which is distinguished by a low-lying π^* orbital localized at the four tetrazine nitrogen atoms.^{8,9} The $4+$ and $5+$ states of **2** were described recently by Johnson, de Groff, and Ruminski.¹⁰ In contrast to the closely related bis(2,2'-bipyridine)ruthenium system (3^{n+}),^{6b,9} the ammine complex 2^{n+} was shown¹⁰ to form a mixed-valent $5+$ state at rather low potentials with a very large comproportionation constant $K_c = \log\{[(E(4+/5+) - E(5+/6+))/0.059 \text{ V}]\}$ of $10^{14.2}$ in water, corresponding to $\Delta E = 840 \text{ mV}$. (The Creutz–Taube ion has $\Delta E = 0.390 \text{ mV}$ and thus $K_c = 10^{6.6}$.)^{2,3} Despite this extremely strong “electrochemical” coupling between the metal centers in 2^{n+} as indicated by the K_c value, there was no indication for an IT band up to 1300 nm.¹⁰ We now report that this transition can be found, albeit in the form of an unexpectedly weak absorption

- (1) (a) Robin, M. B.; Day, P. *Adv. Inorg. Chem. Radiochem.* **1967**, *10*, 247. (b) Brown, D. M., Ed. *Mixed-Valence Compounds*; Reidel: Dordrecht, The Netherlands, 1980. (c) Prassides, K., Ed. *Mixed Valency Systems—Applications in Chemistry, Physics and Biology*; Kluwer: Dordrecht, The Netherlands, 1991.
- (2) (a) Creutz, C. *Prog. Inorg. Chem.* **1983**, *30*, 1. (b) Richardson, D. E.; Taube, H. *J. Am. Chem. Soc.* **1983**, *105*, 40. (c) Richardson, D. E.; Taube, H. *Coord. Chem. Rev.* **1984**, *60*, 107. (d) Tanner, M.; Ludi, A. *Inorg. Chem.* **1981**, *20*, 2348.
- (3) Creutz, C.; Taube, H. *J. Am. Chem. Soc.* **1969**, *91*, 3988; **1973**, *95*, 1086.
- (4) Blasse, G. *Struct. Bonding (Berlin)* **1991**, *76*, 153.
- (5) (a) Schatz, P. N. In ref 1c, p 7. (b) Neuschwander, K.; Piepho, S. B.; Schatz, P. N. *J. Am. Chem. Soc.* **1985**, *107*, 7862. (c) Zhang, L.-T.; Ko, J.; Ondrechen, M. J. *J. Am. Chem. Soc.* **1987**, *109*, 1666. (d) Ondrechen, M. J.; Ko, J.; Zhang, L.-T. *J. Am. Chem. Soc.* **1987**, *109*, 1672.
- (6) (a) Kaim, W.; Kasack, V.; Binder, H.; Roth, E.; Jordanov, J. *Angew. Chem., Int. Ed. Engl.* **1988**, *27*, 1174. (b) Ernst, S.; Kasack, V.; Kaim, W. *Inorg. Chem.* **1988**, *27*, 1146. (c) Kaim, W.; Kasack, V. *Inorg. Chem.* **1990**, *29*, 4696.
- (7) (a) Bruns, W.; Kaim, W. *J. Organomet. Chem.* **1990**, *390*, C45. (b) Bruns, W.; Kaim, W. In ref 1c, p 365. (c) Kaim, W.; Bruns, W.; Poppe, J.; Kasack, V. *J. Mol. Struct.* **1993**, *292*, 221. (d) Bruns, W.; Kaim, W.; Ladwig, M.; Olbrich-Deussner, B.; Roth, T.; Schwederski, B. In *Molecular Electrochemistry of Inorganic, Bioinorganic and Organometallic Compounds*; Pombeiro, A. J. L., McCleverty, J., Eds.; Kluwer: Dordrecht, The Netherlands, 1993; p 255. (e) Bruns, W. Ph.D. Thesis, University of Stuttgart, 1993.

- (8) (a) Kohlmann, S.; Ernst, S.; Kaim, W. *Angew. Chem., Int. Ed. Engl.* **1985**, *24*, 684. (b) Kaim, W.; Kohlmann, S. *Inorg. Chem.* **1987**, *26*, 68.
- (9) (a) Kaim, W.; Ernst, S.; Kohlmann, S.; Welkerling, P. *Chem. Phys. Lett.* **1985**, *118*, 431. (b) Jaradadt, Q.; Barqawi, K.; Akasheh, T. S. *Inorg. Chim. Acta* **1986**, *116*, 63. (c) Ernst, S. D.; Kaim, W. *Inorg. Chem.* **1989**, *28*, 1520. (d) Kaim, W.; Ernst, S.; Kasack, V. *J. Am. Chem. Soc.* **1990**, *112*, 173.
- (10) Johnson, J. E. B.; de Groff, C.; Ruminski, R. R. *Inorg. Chim. Acta* **1991**, *187*, 73.

band, in the near-infrared (near-IR) region; we also present complete UV/vis and EPR spectroelectrochemical results for both of the persistent 5+ and 3+ states. The latter is of interest with respect to the role of the ruthenium coligands in comparison to those in 3²⁺.



Experimental Section

Materials. Although complex 2⁴⁺(PF₆⁻)₄ was obtained essentially according to the literature,¹⁰ the procedure had to be altered in two respects: The gram amount of bptz given in ref 10 is too high by 1 order of magnitude (0.149 mmol corresponds to 0.0353 g), and the volume of the reaction mixture had to be reduced 10-fold to 10 mL in order to ensure precipitation of 2⁴⁺ as the analytically and spectroscopically pure tetrakis(hexafluorophosphate) salt.

For vis/near-IR spectroscopic measurements in DMSO and 1 M DCl/D₂O, the mixed-valent ion 2⁵⁺ was precipitated as a reddish purple salt with mixed bromide/hexafluorophosphate anions by treating the blue Ru(II)/Ru(II) precursor with bromine in ethanol. The identity of the oxidizing 5+ ion was confirmed by comparison with spectroelectrochemically obtained data (see Table I).

Instrumentation. EPR spectra were recorded in the X band on a Bruker ESP 300 spectrometer equipped with a Bruker ER035M gaussmeter and an HP 5350B microwave counter. Cyclic voltammetry was carried out in dry acetonitrile/0.1 M Bu₄NPF₆ using a three-electrode configuration (GCE, Ag/AgCl, Pt) and a PAR 273/175 potentiostat and function generator. Absorption spectra were obtained using a Bruins Instruments Omega 10 spectrometer; the program Lab Calc (Galactic Industries Corp.) was used for spectra deconvolution.

Spectroelectrochemistry. UV/vis/near-IR spectroelectrochemistry was performed in a previously described OTTE (optically transparent thin-layer electrode) cell.¹¹ Electrolyses were carried out at preset potentials until no more spectral changes were observed. The stabilities of the oxidation states were checked by obtaining 100% regeneration of starting material upon reversed electrolysis and by the appearance of isosbestic points. The paramagnetic forms for EPR spectroscopy were generated electrolytically^{9c} or chemically, i.e. using cobaltocene for the reduction of 2⁴⁺.

Results

The electrochemical results for the complex 2⁴⁺(PF₆⁻)₄ in water¹⁰ with two fully spectroelectrochemically reversible (3+/4+/5+) and two cyclovoltammetrically reversible steps (2+/3+, 5+/6+) could essentially be reproduced in acetonitrile, yielding the ΔE and K_c values summarized in Table I. Similarly, the main absorption features of the 4+ ion at 850 (sh), 599, and 367 nm and of the chemically and spectroelectrochemically generated 5+ ion at 518 nm in acetonitrile are very similar to those reported for aqueous solutions;¹⁰ an additional maximum at 347 nm was found for the 5+ form. Three isosbestic points occur at 412, 556, and 1054 nm (Figure 1) for the (4+/5+) equilibrium.

Our experimental facilities have now allowed us to detect two weak long-wavelength absorption bands of 2⁵⁺. One broad band is rather solvent-sensitive, lying at 900 nm in acetonitrile (ϵ 1100 M⁻¹ cm⁻¹), at about 800 nm in DMSO, and below 720 nm in 1 M DCl/D₂O. The other new band at about 1450 nm (Table I) is unsymmetrical (with some visible structuring in aqueous

Table I. Physical Properties of Ligand-Bridged Ruthenium Dimers

	1 ^a	2	3 ^b	
Electrochemical Data ^c				
$E(6+/5+)$	+0.87 (80)	+1.58 (90)	+2.02 (n.d.)	
$E(5+/4+)$	+0.44 (66)	+0.69 (65)	+1.52 (60)	
$E(4+/3+)$	n.d.	-0.75 (70)	-0.03 (60)	
$E(3+/2+)$	n.d.	-1.54 (65)	-1.25 (irr)	
$K_c(3+)$	n.d.	10 ^{13.3}	(ca. 10 ²⁰)	
$K_c(5+)$	10 ^{6.6}	10 ^{15.0}	10 ^{8.5}	
Absorption Data ^d for the 5+ Ions				
$\lambda_{IT}(\tilde{\nu}_{IT})^e$	1560 (6400)	1453 (6880)	n.d.	
ϵ^f	5000	500	n.d.	
$\Delta\nu_{1/2}^g$	1250	ca. 1600	n.d.	
EPR Data ^h				
	1 ⁵⁺	2 ⁵⁺	2 ³⁺	3 ³⁺
g_1	1.346	2.019	1.989	
g_2	2.489	2.418	1.989	n.d.
g_3	2.799	2.913	2.022	
$\langle g \rangle$	2.298	2.477	2.00	1.9980

^a From refs 2, 3, and 14. ^b From refs 9 and 10. ^c From cyclic voltammetry in acetonitrile solutions. Potentials in V vs SCE (1, 3) or Ag/AgCl (2), the potential of SCE being slightly more positive (by 0.02 V) than that of Ag/AgCl. Peak potential differences (in mV) are given in parentheses. n.d. = not determined; irr = irreversible step (peak potential given). $K_c = 10 \exp(\Delta E/0.059 \text{ V})$. ^d In acidic aqueous solution. ^e Absorption maximum in nm (and cm⁻¹). Values for 2⁵⁺ in other solvents: 1433 nm (6980 cm⁻¹, in CH₃CN), 1463 nm (6840 cm⁻¹, in DMSO). ^f Molar extinction coefficient at the absorption maximum in M⁻¹ cm⁻¹. ^g Bandwidth at half-height in cm⁻¹. ^h From measurements at 3 K using a single crystal (1⁵⁺) or a frozen acetonitrile solution (2⁵⁺).

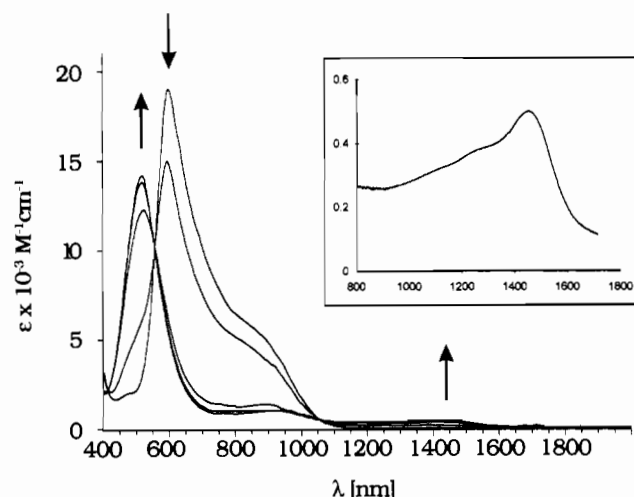


Figure 1. Vis/near-IR spectroelectrochemistry of 2⁴⁺→⁵⁺ in CH₃CN/0.1 M Bu₄NPF₆ at +0.95 V vs Ag/AgCl. The insert shows an enlargement of the near-IR region for 2⁵⁺ in 1 M DCl/D₂O with the unsymmetrical, slightly structured IT band.

solution; Figure 1) and virtually solvent-sensitive with a molar extinction coefficient ϵ of 500 M⁻¹ cm⁻¹ in CH₃CN and 1 M DCl/D₂O solutions (Figure 1).

UV/vis spectroelectrochemistry was also performed for the (4+/3+) couple (Figure 2), yielding absorptions at 745, 559, and 393 nm for the singly reduced form. Spectroelectrochemistry beyond the 3+ and 5+ forms did not produce sufficiently persistent species.

EPR spectra of both the 3+ and 5+ paramagnetic forms could only be observed at low temperatures (<70 K) in frozen acetonitrile solution (Figures 3 and 4). Whereas an axial spectrum with small g anisotropy was observed for 2³⁺, the analogue 2⁵⁺ of the Creutz-Taube ion shows a rhombic EPR signal with all three components above $g = 2$. Figures 3 and 4 illustrate the absence of detectable hyperfine splitting; the g values are summarized in Table I.

(11) Krejčík, M.; Danek, M.; Hartl, F. J. *Electroanal. Chem. Interfacial Electrochem.* 1991, 317, 179.

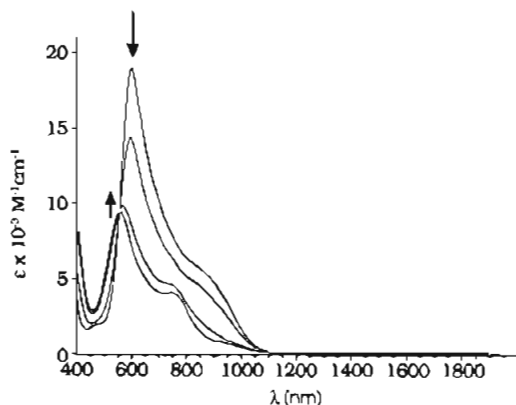


Figure 2. Vis/near-IR spectroelectrochemistry of $2^{4+} \rightarrow 3^{3+}$ in $\text{CH}_3\text{CN}/0.1 \text{ M Bu}_4\text{NPF}_6$ at -1.00 V vs Ag/AgCl .

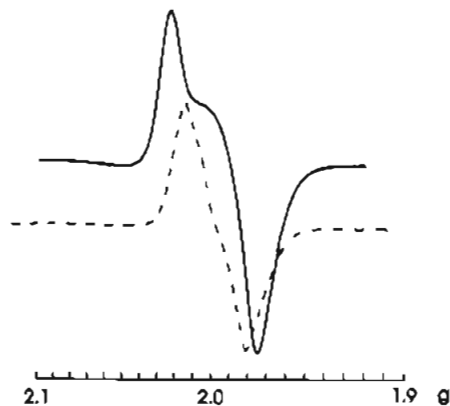


Figure 3. EPR spectra of 2^{3+} (—, at 2.9 K) and 3^{3+} (---, at 3.8 K) in frozen acetonitrile/ $0.1 \text{ M Bu}_4\text{NPF}_6$.

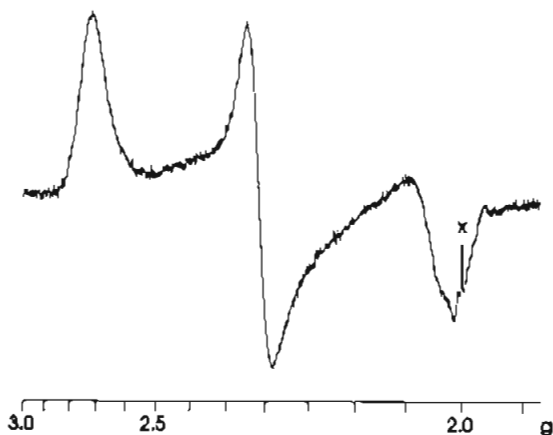
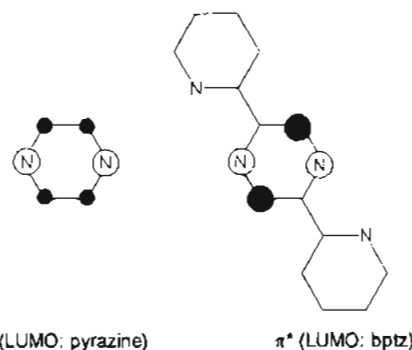


Figure 4. EPR spectrum of electrogenerated 2^{3+} at 3 K in frozen acetonitrile/ $0.1 \text{ M Bu}_4\text{NPF}_6$. Simultaneously detected small amounts of 2^{3+} are indicated (x).

Discussion

The Creutz-Taube system 1^{2+} and the complexes 2^{2+} have in common that the two equivalent ruthenium ammine centers are bridged by six-membered heterocycles which have low-lying π^* orbitals.^{8b,12} The lowest lying unoccupied molecular orbital (LUMO) of bptz is distinguished by a localization of π MO coefficients at the tetrazine nitrogen centers, leaving only a marginal acceptor effect for the pyridyl groups.^{8,9,12} The lower lying π^* level of bptz relative to that of pyrazine in **1** has allowed us to reversibly reduce the ruthenium(II) complex 2^{4+} and study the stable 3^{3+} form; the nature of *both* frontier orbitals could thus be established by EPR and absorption spectroscopy.

(12) The related 2,5-bis(2-pyridyl)pyrazine (bppy) ligand has a LUMO delocalized over the pyridyl rings^{8b} and is thus an electronically less close analogue to pyrazine than bptz.



The EPR studies confirm that the HOMO of 2^{4+} is metal-centered. The isotropic g factor of (g) = 2.477 for 2^{3+} (Table I), derived according to

$$\langle g \rangle = [1/3(g_1^2 + g_2^2 + g_3^2)]^{1/2}$$

is virtually identical with (g) = 2.476 as calculated from $g_{\perp} = 2.722$ and $g_{\parallel} = 1.889$ for a monomeric catecholate complex of tetraammineruthenium(III).¹³ The distinctly rhombic symmetry indicated by the spectrum in Figure 4 reflects the lower symmetry at the metals in 2^{2+} , in relation both to the cited¹³ catecholate complex of $[(\text{NH}_3)_4\text{Ru}]^{3+}$ and to the Creutz-Taube ion (Table I).¹⁴ On the other hand, similarly bis-chelated ruthenium(II,III) dimers with dianionic (O,N-)bridging ligands also show pronounced rhombicity,^{6a,c} albeit with a lower (g) due to considerable ligand participation.^{6c} In comparison to the Creutz-Taube ion 1^{5+} with nonchelated metal centers and an essentially different coordination geometry relative to the π system (see Figure 5), the complex 2^{3+} exhibits a higher isotropic g value but smaller g anisotropy (Table I). Unfortunately, the broad EPR signals did not allow us to determine the amount of (de-)localization on the basis of $^{99,101}\text{Ru}$ hyperfine coupling.^{9a,d,14,15}

For 2^{2+} , the rather small g anisotropy and the occurrence of the components in the vicinity of the free-electron value of 2.0023 (Table I) point to a much smaller contribution from the metal centers to the singly occupied MO.¹⁶ It is thus reasonable to assume that the unpaired electron is confined largely to the tetrazine portion of the bridging ligand as we had unambiguously shown before by hyperfine structure analysis for the related ion 3^{3+} .^{9b,c} The observed axial symmetry (Figure 3) is in agreement with the π^* nature of the singly occupied MO.¹⁶

In contrast to 3^{3+} , the paramagnetic 2^{3+} shows no detectable EPR signal above ca. 70 K, and the g anisotropy is slightly more pronounced. These results point to a stronger mixing of π^* (bptz) and occupied metal d orbitals due to the destabilization of the latter on going from $\text{Ru}(\text{bpy})_2^{2+}$ to $\text{Ru}(\text{NH}_3)_4^{2+}$. In addition, a small amount of spin delocalization to the π^* orbitals of the bpy coligands is conceivable for 3^{3+} although the much lower lying π^* levels of the bptz ligand should preclude electron hopping as was established between equivalent α -diimine sites in $[\text{Ru}(\alpha\text{-diimine})_3]^+$.^{9d,17} Incidentally, Figure 3 shows the first EPR spectrum of a ruthenium(II) ammine complex bound to an anion radical ligand.¹⁸ The instability of protic $\text{Ru}(\text{NH}_3)_n^{2+}$ at negative

(13) Salmonsén, R. B.; Abelleira, A.; Clarke, M. J. *Inorg. Chem.* **1984**, *23*, 385.

(14) Stebler, A.; Ammeter, J. H.; Fürholz, U.; Ludi, A. *Inorg. Chem.* **1984**, *23*, 2764.

(15) Cf. Mn dimers: Gross, R.; Kaim, W. *Inorg. Chem.* **1986**, *25*, 4865.

(16) Kaim, W. *Coord. Chem. Rev.* **1987**, *76*, 187.

(17) (a) Morris, D. E.; Hanck, K. W.; DeArmond, M. K. *J. Am. Chem. Soc.* **1983**, *105*, 3032. (b) Gex, J. N.; DeArmond, M. K.; Hanck, K. W. *J. Phys. Chem.* **1987**, *91*, 251. (c) Gex, J. N.; Cooper, J. B.; Hanck, K. W.; DeArmond, M. K. *J. Phys. Chem.* **1987**, *91*, 4686. (d) Gex, J. N.; Brewer, W.; Bergmann, K.; Tait, C. D.; DeArmond, M. K.; Hanck, K. W.; Wertz, D. W. *J. Phys. Chem.* **1987**, *91*, 4776.

(18) EPR of $[(N\text{-methylpyrazinium})\text{Ru}^{\text{II}}(\text{NH}_3)_3]^{2+}$: Poppe, J.; Kaim, W.; Katz, N. Paper presented at the Eighth Argentinian Congress on Physical Chemistry.

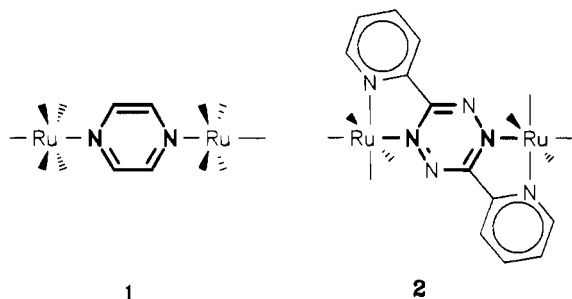
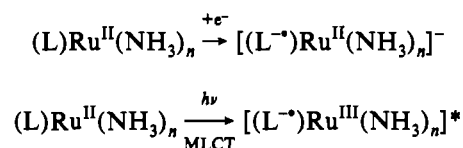


Figure 5. Idealized coordination geometries of systems 1 and 2.

potentials and the apparently rapid EPR relaxation rates make it difficult to observe such spectra although these complexes are interesting because of their model character for corresponding MLCT excited states.



The EPR results thus support the assignment¹⁰ of the long-wavelength absorption bands of the 4+ ions to MLCT transitions ($d\pi \rightarrow \pi^*$). On one-electron reduction, the intensities of the MLCT features decrease to about 50% and shift to slightly higher energies (Figure 2). This is in agreement with the assumption that the essentially nonbonding π^* orbital of bptz is now only half-occupied.

Upon oxidation of 2^{4+} , the main $d\pi \rightarrow \pi^*$ transition shifts to higher energies, as expected.^{2,3,10} However, careful inspection of the near-IR region of the spectrum during oxidative spectroelectrochemistry in acetonitrile also revealed a remaining absorption around 900 nm and a growing weak band at 1450 nm. The former can be attributed to the overlap-forbidden $a_1 \rightarrow b_2$ MLCT transition¹⁹ (cf. the shoulder of the 4+ form),^{9a,10} this assignment being supported by the marked hypsochromic shift in more polar solvents (negative solvatochromism; see Results). On the other hand, we identify the new 1450-nm feature of the 5+ ion as the IT band. Both the virtually solvent-insensitive absorption maximum and the overall width and shape of the band are quite similar to corresponding values for the Creutz-Taube ion,^{2,3,21d} in agreement with a related orbital situation as concerns the bridging ligand. The main difference concerns the intensity, the IT band of 2^{5+} being weaker by an order of magnitude than that of 1^{5+} in either acetonitrile or aqueous solution.

In 1 M DCl/D₂O the high-energy tail of the unsymmetrical IT band can be inspected without disturbing MLCT features (Figure 1). It exhibits two shoulders at about 1280 nm (7810 cm^{-1}) and 1150 nm (8700 cm^{-1} ; from spectra deconvolution), which yields a spacing of about 900 cm^{-1} , presumably due to vibrational splitting.^{5,21} The rigid chelate arrangement in 2^{5+} should favor the observability of such features.

The remarkable decrease of IT band intensity from 1^{5+} to 2^{5+} for an electrochemically much more strongly coupled system must be seen in connection with the difference in orientation between the bridging ligand and the octahedrally coordinated metal centers (Figure 5). The staggered arrangement in complexes $Ru(NH_3)_5(L)$ with nonchelating heteroaromatic ligands L^{20} is

different from the chelate-induced conformation of **2** in which the ruthenium-N(ammine) bonds lie either in the π plane or orthogonal to it; i.e., the bridging π system and the set of ruthenium $4d_{xz}$ ($d\pi$) orbitals⁵ are rotated by 45° against each other relative to the situation in the Creutz-Taube ion.⁵ As a result, the $d\pi$ orbitals of the metals, which are directed toward the middle of the α -diimine chelate system,^{8b,20} are not linearly oriented toward each other^{8b} as in 1^{5+} .^{3,5}

Application of the Hush theory^{2a,21} to the IT spectral data of 2^{5+} yields a bandwidth at half-height, $\Delta\tilde{\nu}_{1/2}$, which is much higher than the experimental value.

$$\Delta\tilde{\nu}_{1/2} = (2310\tilde{\nu})^{1/2} [cm^{-1}]$$

$$\Delta\tilde{\nu}_{1/2}(2^{5+}; calc) = 3990 cm^{-1}$$

$$\Delta\tilde{\nu}_{1/2}(2^{5+}; exp) \approx 2000 cm^{-1}$$

Both the virtual solvent insensitivity of the IT absorption maximum and the above discrepancy strongly suggest that 2^{5+} is a delocalized (class III) system to which the above treatment is not applicable.^{1,2} Accordingly, the degree of electronic coupling, H_{AB} , can be estimated to about $1/2\tilde{\nu} = 3450 cm^{-1}$.²

The huge stability constants K_c for both the 5+ and 3+ forms of **2** deserve a final comment. The stability range for the mixed-valent 5+ state is very large here because of (i) less charge delocalization within $Ru(NH_3)_4^{n+}$ relative to $Ru(bpy)_2^{n+}$,¹⁰ (ii) a conjugated bridging ligand with high LUMO coefficients at the coordination sites,^{6b,8b} and (iii) the rigidity as caused by the chelate arrangement. The stability of the anion-radical state of tetrazines toward disproportionation is not unexpected,^{8b,9a} however, in most previous cases the second reduction step was found to be highly irreversible.^{2,8b,9c,23}

Summarizing, we have shown that 2^{5+} can be unambiguously identified as a delocalized (class III) diruthenium(II,III) mixed-valent system with an unprecedentedly large^{2a} comproportionation constant of $K_c = 10^{15}$ but a rather weak intervalence transition in the near-IR region. The sometimes routinely implied correlation between K_c and the intensity of the IT band is thus valid only for structurally closely analogous systems such as $\{(\mu-\eta^1:\eta^1-L)Ru(NH_3)_3\}_2\}^{5+}$ ($L =$ aromatic N-heterocycles), which represent the majority of ruthenium(II,III) dimers.² Complexes with different coordination arrangements and hence a different extent of metal-ligand orbital overlap do not have to follow such correlations as illustrated by the examples $\{(\mu-NCCN)[Ru(NH_3)_5]\}^{5+}$ ($K_c > 10^{13}$, $\tilde{\nu}_{IT} 6990 cm^{-1}$, $\epsilon 410 M^{-1} cm^{-1}$, $\Delta\tilde{\nu}_{1/2} 1600 cm^{-1}$),²⁴ $\{(\mu-\eta^2:\eta^2-C_6H_6)[Os(NH_3)_5]\}^{5+}$ ($K_c > 10^{8.5}$, $\tilde{\nu}_{IT} 5710 cm^{-1}$, $\epsilon 220 M^{-1} cm^{-1}$, $\Delta\tilde{\nu}_{1/2} 1600 cm^{-1}$),²⁵ and bis chelate complexes of the type $[(\mu-\eta^2:\eta^2-L)(RuL'_n)_2]^n$ ($n = 3+^6$ and $5+$ (this work)).

Acknowledgment. Support from the Deutsche Forschungsgemeinschaft, Volkswagenstiftung, and Fonds der Chemischen Industrie is gratefully acknowledged. We also thank Dr. M. Krejčík (Prague, Czechoslovakia) for introduction to the spectroelectrochemical cell and Professor N. E. Katz (Tucuman, Argentina) for valuable suggestions concerning syntheses.

- (19) Balk, R. W.; Stufkens, D. J.; Oskam, A. *Inorg. Chim. Acta* **1978**, *28*, 133; **1979**, *34*, 267.
 (20) (a) Fürholz, U.; Bürgi, H.-B.; Wagner, F. E.; Stebler, A.; Ammeter, J. H.; Krausz, E.; Clark, R. J. H.; Stead, M. J.; Ludi, A. *J. Am. Chem. Soc.* **1984**, *106*, 121. See also: Gross, M. E.; Creutz, C.; Quicksall, C. O. *Inorg. Chem.* **1981**, *20*, 1522.

- (21) (a) Allen, G. C.; Hush, N. S. *Prog. Inorg. Chem.* **1967**, *8*, 357. (b) Hush, N. S. *Prog. Inorg. Chem.* **1967**, *8*, 391. (c) Hush, N. S. *Coord. Chem. Rev.* **1985**, *64*, 135. (d) Reimers, J. R.; Hush, N. S. In ref 1c, p 29.
 (22) Kaim, W.; Moscherosch, M.; Kohlmann, S.; Field, J. S.; Fenske, D. J. *Chem. Soc., Dalton Trans.*, in press.
 (23) Troll, T. *Electrochim. Acta* **1982**, *27*, 1311.
 (24) Tom, G. M.; Taube, H. *J. Am. Chem. Soc.* **1975**, *97*, 5310.
 (25) Harman, W. D.; Taube, H. *J. Am. Chem. Soc.* **1987**, *109*, 1883.